12th International Symposium on Turbulence and Shear Flow Phenomena (TSFP12)
Osaka, Japan (Online), July 19-22, 2022

QG SIMULATION OF JUPITER'S GREAT RED SPOT WITH DISCRETE EXTERIOR CALCULUS

Pankaj Jagad
Mechanical Engineering, PSE Division
King Abdullah University of Science and Technology
Thuwal, Saudi Arabia
pankaj.jagad@kaust.edu.sa

Ravi Samtaney
Mechanical Engineering, PSE Division
King Abdullah University of Science and Technology
Thuwal, Saudi Arabia
ravi.samtaney@kaust.edu.sa

ABSTRACT

Simulating long lived coherent structures such as the great red spot (GRS) on Jupiter is a challenge from a modeling and a numerical standpoint. Presently, we employ a reduced-gravity quasi geostrophic (QG) formulation to simulate the GRS. Furthermore, we employ a discrete exterior calculus simulation technique. DEC is known to be a robust numerical method with strong structure preserving properties. To setup the physical conditions we decompose the potential vorticity into three parts: one governs the potential vorticity in the zonal flow, while a second part comprises of the potential vorticity in the GRS vortex, and finally an intermediate potential vorticity field which accounts for the deflection of the flow around the GRS. An iterative technique is employed that constraints the potential vorticity to observations of the GRS and zonal flow velocity fields. Preliminary simulations of the GRS on a full spherical surface are presented.

INTRODUCTION

The persistence of the giant vortex, Jupiter's great red spot (GRS), for over three hundred years has been a research topic of interest for not only astrophysicists but also fluid dynamists. Modeling and simulating the GRS can shed some light on its origin as well as longevity. Previous attempts at simulating the GRS have been limited to the β-plane and to a domain size limited to the GRS plus a small neighborhood surrounding the GRS (Shetty *et al.*, 2007). Here, we consider spherical geometry and a domain comprising of the entire spherical surface.

Discrete exterior calculus (DEC) is a robust numerical method with desirable conservation and mimetic properties (Hirani, 2003). Several DEC discretizations of the incompressible Navier-Stokes/Euler equations are known to exactly conserve mass, vorticity and kinetic energy (Mullen *et al.*, 2009; Mohamed *et al.*, 2016). These structure preserving attributes make DEC an appropriate choice for investigating flows dominated by long-lived coherent structures. Moreover, the coordinate independence property of DEC makes is convenient for investigating flows over arbitrary curved surfaces/manifolds. Presently, we develop a method for simulating GRS using a DEC scheme extending our previous work (Jagad *et al.*, 2021).

PHYSICAL SETUP AND NUMERICAL METHOD

We employ 1.5 layer reduced-gravity quasi geostrophic (QG) flow assumption (Ingersoll & Cuong, 1981), wherein a shallow upper layer (containing visible clouds and vortices) of a constant density overlies a much deeper lower layer of a constant density containing the shearing zonal flow. The two layers are dynamically equivalent to a single layer with a rigid bottom topography (parameterizing the flow in the lower layer) and an effective gravity. The computational domain consists of a spherical surface rotating about its north-south axis. The governing equation for the system conserves potential vorticity written as follows.

$$\frac{\partial q}{\partial t} + \mathbf{u} \cdot \nabla q = 0, \tag{1}$$

where q is the potential vorticity and $\mathbf{u}$ is the velocity vector. The potential vorticity is expressed as

$$q(\theta,\phi,t) = \left(\nabla^2 - \frac{1}{L_R^2}\right)\psi(\theta,\phi,t) + f(\theta) + \frac{h_b(\theta)\,g}{f_o L_R^2}, \tag{2}$$

where ψ is the stream function, L_R is the Rossby deformation radius, h_b is a function of latitude/colatitude representing the bottom topography, g is the reduced/effective gravity, f is the Coriolis parameter, and f_0 is the Coriolis parameter at a reference location. The Rossby deformation radius $L_R = \sqrt{gH_o}/f_o$, (H_0 is the mean height of the layer) is a length scale at which the Coriolis force becomes comparable to pressure forces associated with the hydrostatic equilibrium. The Coriolis parameter $f(\theta) \equiv 2\Omega\cos\theta$, where Ω is the rate of rotation of the domain and θ is the colatitude. The GRS drifts westward with nearly a constant velocity, and in a frame of reference translating with GRS, the QG equations (1) - (2) have a steady

solution $q(\theta,\phi)$. Therefore, in a similar approach as Shetty *et al.* (2007), we decompose the total potential vorticity into three components as follows:

$$q(\theta,\phi) = q^{\infty}(\theta) + q^{\mathrm{GRS}}(\theta,\phi) + q^{\mathrm{INT}}(\theta,\phi), \tag{3}$$

where q^{∞} is the potential vorticity in the zonal flow, q^{GRS} is the potential vorticity in the GRS vortex, and q^{INT} is the potential vorticity which accounts for the deflection of the flow around GRS, and vanishes asymptotically into and away from GRS. These components can further be expressed as:

$$q^{\mathrm{GRS}} = \left(\nabla^2 - \frac{1}{L_R^2}\right)\psi^{\mathrm{GRS}}, \tag{4}$$

$$q^{\infty} = \left(\nabla^2 - \frac{1}{L_R^2}\right)\psi^{\infty} + f + \frac{h_b(\theta)\,g}{f_o L_R^2}, \tag{5}$$

$$q^{\mathrm{INT}} = \left(\nabla^2 - \frac{1}{L_R^2}\right)\psi^{\mathrm{INT}}. \tag{6}$$

We employ the observations of the GRS and zonal flow velocity fields (Mitchell *et al.*, 1981; Limaye, 1986), and with the GRS superimposed on the zonal flow, we compute the corresponding potential vorticity distribution as an initial guess. To this end, we compute q^{GRS} directly from equation (4), and compute q^{∞} as follows. For the zonal flow, we compute the Bernoulli function (B) distribution as

$$\left(\nabla^2\psi^{\infty} + f\right)\hat{e_r} \times \mathbf{u}^{\infty} = -\nabla B, \tag{7}$$

where $\mathbf{u}^{\infty}$ is the zonal flow velocity field. We subtract the kinetic energy from it to arrive at the potential energy distribution gh. Next, we compute $q^{\infty} = \frac{L_R^2 f_0^2(\omega+f)}{gh}$, where ω is the relative vorticity. Then, we compute the product of the bottom topography function and the reduced gravity distribution via equation (5). We assume the GRS center as the reference location for the computation of f_0. The potential vorticity distribution computed from the superposition of the GRS on the zonal flow does not conserve advectively, because it does not account for the deflection of flow around the GRS. Therefore, it is updated using an iterative procedure as follows. In a frame translating with the GRS, for a current velocity field, we compute the updated potential vorticity that is advectively conserved. Finally, we update the stream function by inverting the Helmholtz equation (2), and repeat the procedure until the flow field converges to a steady solution. An alternative approach is to solve the governing momentum and continuity equations in primitive variables as follows.

$$\frac{\partial \mathbf{u}}{\partial t} + \mathbf{u}\cdot\nabla\mathbf{u} = -g\nabla h + f(\theta)\,\mathbf{u}\times\hat{e_r}, \tag{8}$$

$$\nabla\cdot\mathbf{u} = 0. \tag{9}$$

Here, we compute the potential energy term (gh) as

$$gh = f_0\psi - gh_b, \tag{10}$$

where the bottom topography term gh_b is determined as already discussed before. We use the aforementioned initial condition (see figure 4), and let the flow field evolve to a steady state.

RESULTS AND DISCUSSION

Figure 1 shows the distribution of q^{GRS}. It reveals that q^{GRS} is the superposition of four nested patches of nearly uniform potential vorticity, which is in contrast to the assumption of two nested patches for a model of q^{GRS} in the previous work of Shetty *et al.* (2007). Our computation shows two additional narrow patches, the inner most and the outer most, whereas the two intermediate patches are similar to that in Shetty *et al.* (2007). Figure 2 shows the distribution of q^{∞}, and figure 3 shows its profile as a function of the colatitude. The computed zonal flow potential vorticity comprises of nearly homogenized bands, with each band separated from the adjacent ones by a steep meridional gradient of potential vorticity. The profile of zonal flow potential vorticity has the appearance of a staircase, and q^{∞} varies from the north to the south pole non-monotonically. Figure 4 shows the initial potential vorticity distribution computed from the superposition of the GRS on the zonal flow. Figure 5 shows the distribution of total potential vorticity after 5.5 hours (equivalent to 0.26 eddy turnover time), which is still evolving. We will examine the flow physics of GRS for much longer simulations times in the future.

REFERENCES

Dowling, Timothy E & Ingersoll, Andrew P 1989 Jupiter's great red spot as a shallow water system. *Journal of Atmospheric Sciences* **46** (21), 3256–3278.

Hirani, Anil N 2003 Discrete exterior calculus. PhD thesis, California Institute of Technology.

Ingersoll, Andrew P & Cuong, PG 1981 Numerical model of long-lived jovian vortices. *Journal of Atmospheric Sciences* **38** (10), 2067–2076.

Jagad, Pankaj, Abukhwejah, Abdullah, Mohamed, Mamdouh & Samtaney, Ravi 2021 A primitive variable discrete exterior calculus discretization of incompressible navier–stokes equations over surface simplicial meshes. *Physics of Fluids* **33** (1), 017114.

Kwon, O. K. & Pletcher, R. H. 1981 Prediction of the incompressible flow over a rearward-facing step. Technical Report HTL-26, CFD-4. Iowa State Univ., Ames, IA.

Lee, Y., Korpela, S. A. & Horne, R. N. 1982 Structure of multicellular natural convection in a tall vertical annulus. In *Proceedings of 7th International Heat Transfer Conference* (ed. U. Grigul et al.), , vol. 2, pp. 221–226. Washington, D.C.: Hemisphere Publishing Corp.

Limaye, Sanjay S 1986 Jupiter: New estimates of the mean zonal flow at the cloud level. *Icarus* **65** (2-3), 335–352.

Mitchell, Jim L, Beebe, Reta F, Ingersoll, Andrew P & Garneau, Glenn W 1981 Flow fields within jupiter's great red spot and white oval bc. *Journal of Geophysical Research: Space Physics* **86** (A10), 8751–8757.

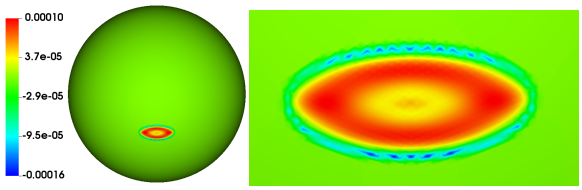

Figure 1. GRS potential vorticity distribution as computed from equation (4) and the observed GRS velocity field, and zoomed in view of GRS showing the details.

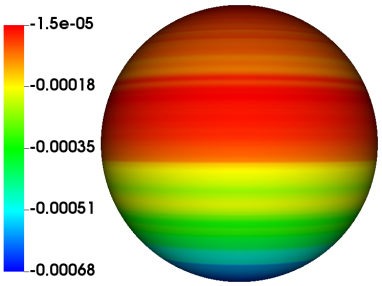

Figure 2. Zonal flow potential vorticity distribution as computed from the aforementioned procedure and the observed zonal flow velocity field

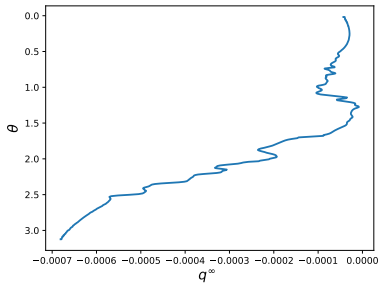

Figure 3. Zonal flow potential vorticity as a function of colatitude. There are nearly homogenized bands of potential vorticity organized into staircase.

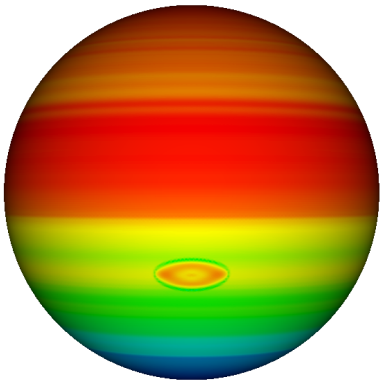

Figure 4. Potential vorticity distribution as computed from the superposition of GRS on the zonal flow.

Mohamed, Mamdouh S, Hirani, Anil N & Samtaney, Ravi 2016 Discrete exterior calculus discretization of incompressible navier–stokes equations over surface simplicial meshes. *Journal of Computational Physics* **312**, 175–191.

Mullen, Patrick, Crane, Keenan, Pavlov, Dmitry, Tong, Yiying & Desbrun, Mathieu 2009 Energy-preserving integrators for fluid animation. *ACM Transactions on Graphics (TOG)* **28** (3), 1–8.

Shetty, Sushil, Asay-Davis, Xylar S & Marcus, Philip S 2007 On the interaction of jupiters great red spot and zonal jet streams. *Journal of the Atmospheric Sciences* **64** (12), 4432–4444.

Sparrow, E. M. 1980*a* Fluid-to-fluid conjugate heat transfer for a vertical pipe - internal forced convection and external natural convection. *ASME Journal of Heat Transfer* **102**, 402–407.

Sparrow, E. M. 1980*b* Forced-convection heat transfer in a duct having spanwise-periodic rectangular protuberances. *Numerical Heat Transfer* **3**, 149–167.

Tung, C. Y. 1982 Evaporative heat transfer in the contact line of a mixture. PhD thesis, Rensselaer Polytechnic Institute, Troy, NY.

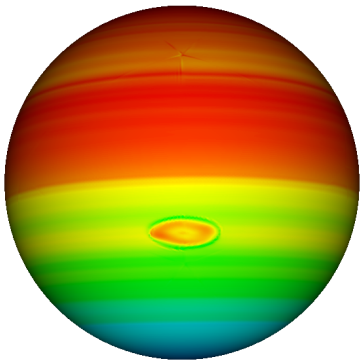

Figure 5. Potential vorticity distribution after 5.5 hours (equivalent to 0.26 eddy turnover time).